Chemistry Europe
European Chemical Societies Publishing

Enantiopure Polyradical Tetrahedral $Pd_{12}L_6$ Cages

Prabhakaran Rajasekar,[a] Abinash Swain,[c] Gopalan Rajaraman,*[c] and Ramamoorthy Boomishankar*[a, b]

Abstract: The synthesis of cages with a polyradical framework remains a challenging task. Herein is reported an enantiomeric pair of quinoid-bridged polyradical tetrahedral palladium(II) cages that are stabilized by an unusual dianionic diradical form ($dhbq^{\bullet\bullet 2-}$). These cages have been characterized by electron paramagnetic resonance and UV-visible spectroscopy, squid magnetometry and mass spectrometry. Single-crystal-derived X-ray investigations of the iso-structural cages built on fluoranilate linkers confirm the tetrahedral structure of the obtained radical cages. Theoretical calculations showed that the diradical state of the dhbq anions is more stable than the usual monoradical state. A weak ferromagnetic exchange between adjacent radical centers was observed in DFT studies.

Metal-organic polyhedral assemblies are an interesting class of coordination compounds due to their capabilities for host-guest chemistry, molecular recognition and separation, as molecular reaction vessels and as support platforms for biologically relevant transformations.[1] Over the years, a large number of cages are synthesized with cationic, anionic and neutral framework structures.[2,3] Molecules possessing polyradical sites are attractive for their redox activities, charge-transfer characteristics and long-range electronic communications that make them potential candidates for electrical conductors, optoelectronic materials and molecular magnets.[4] Anilic acid based dianion derived from deprotonation of 2,5-Dihydroxy benzoquinone ($dhbq^{2-} = [C_6O_4H_2]^{2-}$) is an interesting redox reagent and resembles transition metal ions for the similarities in the energetics of their frontier orbitals.[5] It can undergo either one electron oxidation or two one electron reductions to yield species of charges from −1 to −4 in which the species with −1 and −3 charges yield the persistent radicals. Notably, the radical form of $(C_6H_2O_4)^{\bullet 3-}$ (abbreviated as $dhbq^{\bullet 3-}$), that is found in several mixed-valent metal organic frameworks, show enhanced electrical conductivities, strong magnetic coupling and exhibit inter-valance charge-transfer bands in their electronic spectra.[6] However, such polyradical frameworks are found to be very rare for discrete and polyhedral cage assemblies for the $dhbq^{n-}$ anions, although there are a few reports known based on stable verdazyl radicals or highly reactive TTF-based radicals.[7,8] In fact, the nonradical $dhbq^{2-}$ form prevails most often for heavier divalent transition metal ions to yield diamagnetic discrete self-assemblies possibly due to the presence of additional redox innocent co-ligands in them.[9,10]

In an interesting report, Sato and co-workers have demonstrated an elegant chirality-assisted switching of polarization in a heterometallic [CrCo] complex.[11] Inspired by this finding, we set out to explore the existence of a chiral polyradical framework in the tetrahedral imido-Pd_3 cages by employing various substituted anilate linkers. Herein, we report an enantiomeric pair of polyradical Pd^{II} cages of formula $\{Pd_3[PO(N(^{RRR}CH(CH_3)Ph)_3]\}_4(C_6O_4H_2)_6$ (**1-R**) and $\{Pd_3[PO(^{SSS}CH(CH_3)Ph)_3]\}_4(C_6O_4H_2)_6$ (**1-S**) that have an unusual diradical ($dhbq^{\bullet\bullet 2-}$) form for the anilate ions. The EPR measurements reveal that both **1-R** and **1-S** exhibit six pairs of identical diradical spin centers. The magnetic measurements on **1-S** gave a paramagnetic $\chi_m T$ value of 5.4 $cm^3\,K\,mol^{-1}$ due to 12 unpaired electrons. The theoretic spin density analyses of **1-S** display weak ferromagnetic interactions between the two adjacent radical linkers. To the best of our knowledge, these are the first examples of chiral polyradical frameworks that are ever known for the discrete or polyhedral cage compounds with the elusive $dhbq^{\bullet\bullet 2-}$ edges.

The spin-cages **1-R** and **1-S** were synthesized in a direct reaction involving the corresponding chiral ligands $X^{RRR}H_3$ and $X^{SSS}H_3$, palladium(II) acetate and dhbq-2H in methanol in about 80% yields (Scheme 1). The formation of the cage assemblies **1-R** and **1-S** were confirmed by the MALDI-TOF spectrometry, which unveiled a single peak at *m/z* 3760 corresponding to their $[M+K]^+$ species (Figures S1 and S2 in the Supporting Information). The ^{31}P NMR of **1-R** and **1-S** in $CDCl_3$ displayed a singlet at 70.14 ppm that confirms the presence of the pure cage (Figure S3 and S4). The ^1H NMR analysis of **1-R** and **1-S** revealed broad signals for the protons of the α-methyl benzyl groups attached to the tris(imido) phosphate ligand at the Pd_3 PBUs (Figure S5). The signal broadening is ascribed to the presence of paramagnetic species in the cage framework. The solid-state ^{13}C NMR spectrum showed the presence of carbonyl groups ($\delta = 187$, 192 ppm) and C–H fragments ($\delta = 100$ ppm) of the dhbq linkers in addition to the carbon atoms of the imido-

[a] Dr. P. Rajasekar, Prof. Dr. R. Boomishankar
Department of Chemistry
Indian Institute of Science Education and Research Pune
Pune 411008 (India)
E-mail: boomi@iiserpune.ac.in

[b] Prof. Dr. R. Boomishankar
Centre for Energy Science
Indian Institute of Science Education and Research Pune
Dr. Homi Bhabha Road, Pune 411008 (India)

[c] A. Swain, Prof. Dr. G. Rajaraman
Department of Chemistry
Indian Institute of Technology
Bombay, Mumbai 400076 (India)
E-mail: rajaraman@chem.iitb.ac.in

Supporting information for this article is available on the WWW under https://doi.org/10.1002/chem.202101239

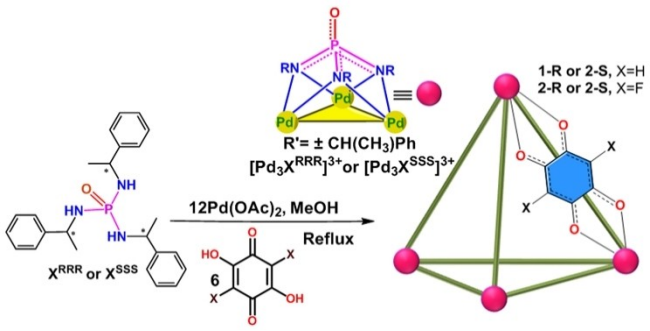

Scheme 1. Synthesis of chiral spin (**1-R**, **1-S**) and neutral (**2-R**, **2-S**) tetrahedral cages from enantiopure $X^{RRR}H_3$ or $X^{SSS}H_3$ ligands. Only one of the six anilate linkers present in these cages is indicated for simplicity.

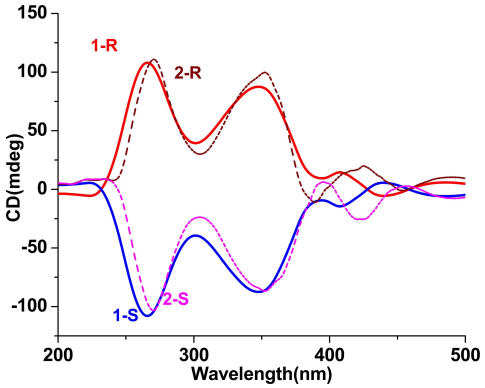

Figure 1. The CD spectra of **1-R**, **1-S**, **2-R** and **2-S**.

phosphate ligands in the cage framework (Figures S6 and S7). The ^{1}H-2D-diffusion-ordered NMR spectroscopy (DOSY) of **1-R** and **1-S** gave diffusion coefficient (*D*) values of 7.32×10^{-10} and 7.533×10^{-10} m^2s^{-1}, respectively, confirming the presence of only one species in solution (Figures S8 and S9). The minor disparity in the observed diffusion coefficients for **1-R** and **1-S** could be due the broad nature of ^{1}H NMR signals monitored in the DOSY experiments. Thermo gravimetric analysis (TGA) data for **1-R** and **1-S** reveals the absence of solvate molecules inside their cage cavities and shows thermal stability upto 200 °C (Figure S10).

Several attempts to crystallize the polyradical cages **1-R** and **1-S** went unsuccessful. Thus, we employed a similar ligand motif based on fluoranilic acid in reaction with the corresponding chiral phosphoramide ligands and $Pd(OAc)_2$ to build isostructural cages **2-R** and **2-S** (yields ~83%). Formation of the tetrahedral cages of formula $\{Pd_3[PO(N(^{RRR}CH(CH_3)Ph)_3]\}_4(C_6O_4F_2)_6$ (**2-R**) and $\{Pd_3[PO(^{SSS}CH(CH_3)Ph)_3]\}_4(C_6O_4F_2)_6$ (**2-S**) has been confirmed by mass spectral analysis (Figure S11 and S12). Unlike **1-R** and **1-S**, **2-R** and **2-S** were found to be diamagnetic as revealed by its ^{1}H NMR analysis that gave clear resonances for the α-methyl benzyl groups (Figures S13 and S14). Their ^{19}F and ^{31}P NMR spectra showed a singlet at −171.41 and 70.34 ppm, respectively (Figures S15 and S16).

The solid state UV-visible spectra of these cages show bands at 339 and 563 nm (for **1-R** and **1-S**) and 345 and 584 nm (for **2-R** and **2-S**) due to d-d and LMCT transitions, respectively (Figure S17). The circular dichroism (CD) spectra of **1-R** and **1-S** gave mirror image signals at 260 and 353 nm due to the respective ligand-centred and ligand to metal charge transfer transitions showing the enantio-enriched nature of the radical cages (Figure 1). The absolute configurations ($[\alpha]^2D$) of **1-R** and **1-S** were found to be 1322° and −1340° in 0.1 M solution of $CHCl_3$ as determined by the optical rotation measurements. The enantio-enriched nature of **2-R** and **2-S** were also confirmed by CD measurements as they show four bisignate bands at 262 (π-π*), 356 (π-π*), 428 (LMCT) and 503 nm (LMCT; Figure 1). The $[\alpha]^2_D$ values of **2-R** and **2-S** were measured to be +1470° and −1430°, respectively.

Crystals of **2-R** and **2-S** suitable for single-crystal X-ray diffraction analysis were obtained from their corresponding dichloromethane solutions. Both of their structures were solved in the orthorhombic chiral space group $P2_12_12$ (Figure 2). The asymmetric units of **2-R** and **2-S** possess one fourth of the cage molecule (Figures S18-S19 and Table S2, S3). The structural analysis confirmed the enantiopure nature of these cages. The tetrahedral cages in **2-R** and **2-S** are a build-up of trigonal Pd_3X^* ($X^* = {}^{RRR/SSS}CH(CH_3)Ph)_3$) chiral units at each of their four corners. The bis-bidentate fluoranilate dianions tether them across the six edges of the tetrahedron via its wide-angle chelating O,O-coordination to the 90° cisoidal sites. Every single Pd_3 unit is cis-protected by the hexadentate coordination of tris(amino) phosphate trianion along the exteriors of the cage. These cages further exhibit a rotational chirality as observed by the clockwise (in **2-R**) or anticlockwise (in **2-S**) orientation of the α-Me groups attached to the chiral carbon centers. The intrinsic void volumes of these cages were found to be 238 Å^3, as indicated by MSROLL calculations.[12] The packing structure of these cages exhibits solvent accessible voids of volume 651 Å^3 which amounts to 6.6% of the total unit cell volume (Figures S20 and S21).

The room temperature EPR spectrum of **1-R** and **1-S** in the solid state displays a single sharp signal at g = 2.002 suggesting presence of unpaired electron(s). This indicates the presence of

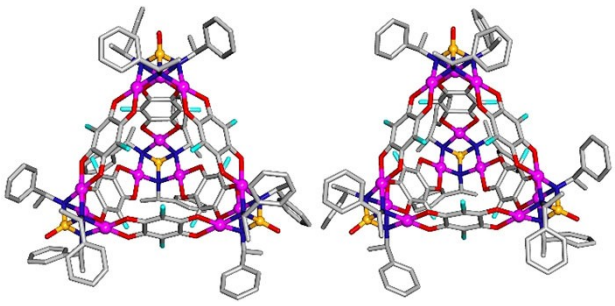

Figure 2. The molecular structures of **2-S** (right) and **2-R** (left); Pd: magenta, P: yellow, C: gray, N: blue, O: red, F: cyan. The hydrogen atoms are omitted for clarity.

a unique radical species within the polyradical cage framework (Figure 3a,b). The intensities of the EPR signals were found to increase upon lowering the temperature from 270 to 100, suggesting a paramagnetic ground state for both of them (Figures 3c and S22). The observation of the forbidden transition confirms the existence of the integer spin state ($\Delta ms = 2$ for example) at half the field (1600 mT) of the main signal (~3200 mT) at 100 K for both **1-R** and **1-S** (Figure 3a, b).

The variable temperature DC magnetic susceptibility measurements on **1-S** gave a room temperature (293 K) $\chi_m T$ value of 5.4 $cm^3\,K\,mol^{-1}$ at 1000 Oe (Figure 3d). The obtained magnetic moment value is consistent with the computed spin-only value for the 12 unpaired electrons ($\chi_m T$ calcd = 4.49 $cm^3\,K\,mol^{-1}$). This confirms the polyradical framework of 12 unpaired electrons is located along the six edges of the tetrahedron. In contrast, the

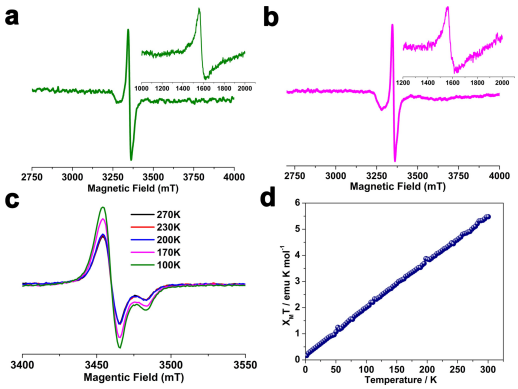

Figure 3. EPR spectra of chiral spin cages a) **1-R** and b) **1-S** along with their forbidden transition at 1600 mT (insets). c) Variable-temperature EPR spectra of **1-S**. d) $\chi_M T$ vs. *T* plot for **1-S**.

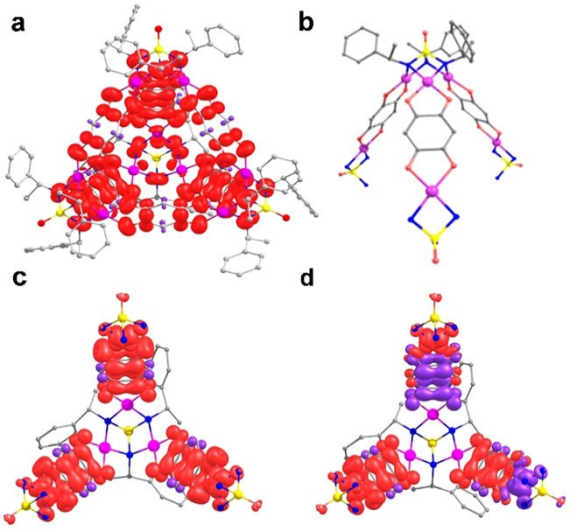

Figure 4. a) DFT-optimized structure of **1-S** showing the spin densities in the high-spin state. b) The idealized repeat unit of **1-S** employed for the calculations. Spin density plots obtained for the repeat unit of **1-S** on c) high- and d) low-spin state that yield the spin-exchange values. Atom color codes: Pd: magenta, P: yellow, C: gray, N: blue, O: red, H: white. The hydrogen atoms are omitted for clarity.

cages **2-R** and **2-S** and their corresponding analogues based on chloranilate linkers $\{Pd_3[PO(N(^{RRR}CH(CH_3)Ph)_3]\}_4(C_6O_4Cl_2)_6$ (**3-R**) and $\{Pd_3[PO\ (^{SSS}CH(CH_3)Ph)_3]\}_4(C_6O_4Cl_2)_6$ (**3-S**) were found to be diamagnetic as indicated by their NMR, EPR and magnetic studies. This confirms the presence of the usual form of the $dhbq^{2-}$ species in them, as observed for most of the anilate complexes of heavier transition metal ions. Also, the presence of electronegative halide substituents on the anilate backbone helps in stabilizing the diamagnetic state of these ligands by withdrawing the spin-densities towards themselves.

As the molecular structures of **1-R** and **1-S** could not be obtained by crystallography, the geometry of **1-S** was optimized using density functional methods by taking the structure of **2-S** as the starting point.[13] Based on the experimental inputs and earlier studies, two scenarios were considered, i) a monoradical $dhbq^{\bullet 3-}$ form and ii) the diradical $dhbq^{\bullet\bullet 2--}$ form for the dhbq-linker moieties in **1-S** (Figures 4a and S23, Table S4). The computed energetics (see Computational Details) reveal that the diradical state is lower in energy in comparison with the monoradical state by 67 $kcal\,mol^{-1}$ per dhbq-site (Figure S24 and Table S3).

To gain insights into the magnetic behaviour of **1-S**, exchange coupling between the two radical centres via Pd^{II} atoms were probed. To estimate this exchange interaction, two sets of calculations were performed. In the first one, an S = 6 state was imposed on the full structure of **1-S**, and in the second one, an S = 0 was calculated where the spins at the alternative radical centres are kept at the opposite directions (keeping each $dhbq^{\bullet\bullet 2-}$ as triplets). An overall ferromagnetic type radical-radical interactions via the Pd^{II} atoms with a coupling constant (*J*) value of $+132\ cm^{-1}$ was obtained from these calculations. From the spin-density plots, it is evident that the unpaired electrons are mostly delocalized on the O–C–C–O moiety of the dhbq ligand and with a small spin density on the Pd^{II} atoms (Figure 4a). Thus, the competing antiferromagnetic and ferromagnetic interactions in the **1-S** has led to a paramagnetic behaviour with a steep decrease in susceptibility, as shown in Figure 3d.

Similar calculations were also performed on a small model system constructed from the idealized repeat unit of **1-S** (Figure 4b–d). These calculations also gave a ferromagnetic coupling between the adjacent spin centres, albeit, with a significant reduction in magnitude for *J* ($+28.5\ cm^{-1}$). To understand the difference in magnetic properties of **1-S** with the other two diamagnetic cages, calculations were also performed on the smaller fragment models taken from the X-ray structures of **2-S** and **3-S** (Figures S25–S26). However, the exchange between the neighboring spin-centers via the Pd^{II} atoms was found to be antiferromagnetic for both **2-S** and **3-S** with the *J* values of -126 and $-420\ cm^{-1}$, respectively. Given the fact that the computed *J* values in these model systems are significantly underestimated, they are expected to be strongly antiferromagnetic for **2-S** and **3-S** rendering a diamagnetic behavior for both of them.

In summary, by employing anilate linkers and Pd^{II} ions, chiral metal-organic cages with polyradical frameworks have been built. Whereas cages based on the dhbq-linker form stable

radical pairs, the fluoranilate- and chloraniate-tethered tetrahedral cages were found to be diamagnetic in nature. The formation of tetrahedral cage assemblies was confirmed by MALDI-TOF and ^{31}P NMR spectroscopy and single-crystal X-ray diffraction analysis of the iso-structural cages based on fluoranilate linkers. Furthermore, the EPR, magnetic measurements and theoretical calculations show the presence of an unusual diradical dianionic form in each of the dhbq$^{\bullet\bullet 2-}$ linkers in these chiral cages. The exchange interactions computed by DFT methods showed the existence of ferromagnetic coupling between adjacent diradical centers via the Pd^{II} atoms for **1-S**, whereas for **2-S** and **3-S**, the exchange was found to be antiferromagnetic in nature. Finally, the present work provides insights into the design and synthesis of stable cage frameworks containing polyradical structures that have enormous potential in the area of spin-electronic devices and catalysis.

Deposition numbers 2074205, and 2074206 contain the supplementary crystallographic data for this paper. These data are provided free of charge by the joint Cambridge Crystallographic Data Centre and Fachinformationszentrum Karlsruhe Access Structures service.

Acknowledgements

This work was supported by SERB, India through grant no. CRG/2019/004615 (R.B.). P.R. thanks the UGC, India. G.R. thanks DST (DST/SJF/CSA-03/2018-10) and SERB (CRG/2018/000430; SB/SJF/2019-20/12; SPR/2019/001145) for funding. We thank Dr. Vekatasubhaih Krishnan for VT-EPR measurements, Dr. Sunil Nair for the magnetic data and Prof. Maheshwaran Shanmugam for valuable discussions.

Conflict of Interest

The authors declare no conflict of interest.

Keywords: cages · chirality · palladium · P–N ligands · radicals

[1] a) H. Amouri, C. Desmarets, J. Moussa, *Chem. Rev.* **2012**, *112*, 2015–2041; b) M. D. Ward, P. R. Raithby, *Chem. Soc. Rev.* **2013**, *42*, 1619–1636; c) M. M. J. Smulders, I. A. Riddell, C. Browne, J. R. Nitschke, *Chem. Soc. Rev.* **2013**, *42*, 1728–1754; d) K. Harris, D. Fujita, M. Fujita, *Chem. Commun.* **2013**, *49*, 6703–6712; e) M. Han, D. M. Engelhard, G. H. Clever, *Chem. Soc. Rev.* **2014**, *43*, 1848–1860; f) M. Han, D. M. Engelhard, G. H. Clever, *Chem. Soc. Rev.* **2014**, *43*, 1848–1860; g) P. Rajasekar, S. Pandey, H. Paithankar, J. Chugh, A. Steiner, R. Boomishankar, *Chem. Commun.* **2018**, *54*, 1873–1876; h) A. M. Castilla, W. J. Ramsay, J. R. Nitschke, *Acc. Chem. Res.* **2014**, *47*, 2063–2073; i) T. R. Cook, P. J. Stang, *Chem. Rev.* **2015**, *115*, 7001–7045.

[2] a) A. V. Davis, D. Fiedler, M. Ziegler, A. Terpin, K. N. Raymond, *J. Am. Chem. Soc.* **2007**, *129*, 15354–15363; b) D. Fiedler, D. H. Leung, R. G. Bergman, K. N. Raymond, *J. Am. Chem. Soc.* **2004**, *126*, 3674–3675; c) M. Ziegler, A. V. Davis, D. W. Johnson, K. N. Raymond, *Angew. Chem. Int. Ed.* **2003**, *42*, 665–668; *Angew. Chem.* **2003**, *115*, 689–692; d) C. Zhao, Q.-F. Sun, W. M. Hart-Cooper, A. G. DiPasquale, F. D. Toste, R. G. Bergman, K. N. Raymond, *J. Am. Chem. Soc.* **2013**, *135*, 18802–18805; e) C. Zhao, F. D. Toste, K. N. Raymond, R. G. Bergman, *J. Am. Chem. Soc.* **2014**, *136*, 14409–14412.

[3] a) R. W. Saalfrank, H. Maid, A. Scheurer, F. W. Heinemann, R. Puchta, W. Bauer, D. Stern, D. Stalke, *Angew. Chem. Int. Ed.* **2008**, *47*, 8941–8945; *Angew. Chem.* **2008**, *120*, 9073–9077; b) R. W. Saalfrank, N. Löw, B. Demleitner, D. Stalke, M. Teichert, *Chem. Eur. J.* **1998**, *4*, 1305–1311; c) T. Liu, Y. Liu, W. Xuan, Y. Cui, *Angew. Chem. Int. Ed.* **2010**, *49*, 4121–4124; *Angew. Chem.* **2010**, *122*, 4215–4218; d) J. L. Bolliger, A. M. Belenguer, J. R. Nitschke, *Angew. Chem. Int. Ed.* **2013**, *52*, 7958–7962; *Angew. Chem.* **2013**, *125*, 8116–8120; e) A. K. Gupta, A. Yadav, A. K. Srivastava, K. R. Ramya, H. Paithankar, S. Nandi, J. Chugh, R. Boomishankar, *Inorg. Chem.* **2015**, *54*, 3196–3202.

[4] a) M. Kurmoo, *Chem. Soc. Rev.* **2009**, *38*, 1353–1379; b) P. Dechambenoit, J. R. Long, *Chem. Soc. Rev.* **2011**, *40*, 3249–3265; c) E. Coronado, G. M. Espallargas, *Chem. Soc. Rev.* **2013**, *42*,1525–1539; d) S. Bivaud, J.-Y. Balandier, M. Chas, M. Allain, S. Goeb, M. Sallé, *J. Am. Chem. Soc.* **2012**, *134*, 11968–11970; e) S. Bivaud, J.-Y. Balandier, M. Chas, M. Allain, S. Goeb, M. Sallé, *J. Am. Chem. Soc.* **2012**, *134*, 11968–11970; f) S. Bivaud, J.-Y. Balandier, M. Chas, M. Allain, S. Goeb, M. Sallé, *J. Am. Chem. Soc.* **2012**, *134*, 11968–11970.

[5] a) S. Kitagawa, S. Kawata, *Coord. Chem. Rev.* **2002**, *224*, 11; b) D. Guo, J. K. McCusker, *Inorg. Chem.* **2007**, *46*, 3257.

[6] a) C. G. Pierpont, L. C. Francesconi, *Inorg. Chem.* **1977**, *16*, 2367; b) A. Dei, D. Gatteschi, L. Pardi, U. Russo, *Inorg. Chem.* **1991**, *30*, 2589; c) M. D. Ward, *Inorg. Chem.* **1996**, *35*, 1712; d) K. S. Min, A. L. Rheingold, A. DiPasquale, J. S. Miller, *Inorg. Chem.* **2006**, *45*, 6135; e) K. S. Min, A. G. DiPasquale, J. A. Golen, A. L. Rheingold, J. S. Miller, *J. Am. Chem. Soc.* **2007**, *129*, 2360; f) K. Min, A. G. DiPasquale, A. L. Rheingold, H. S. White, J. S. Miller, *J. Am. Chem. Soc.* **2009**, *131*, 6229.

[7] a) K. Nakabayashi, Y. Ozaki, M. Kawano, M. Fujita, *Angew. Chem. Int. Ed.* **2008**, *47*, 2046–2048; *Angew. Chem.* **2008**, *120*, 2076–2078; b) Y. Ozaki, M. Kawano, M. Fujita, *Chem. Commun.* **2009**, 4245–4247.

[8] a) S. Goeb, S. Bivaud, P. I. Dron, J.-Y. Balandier, M. Chasa, M. Sallé, *Chem. Commun.* **2012**, *48*, 3106–3108; b) S. Bivaud, J.-Y. Balandier, M. Chas, M. Allain, S. Goeb, M. Sallé, *J. Am. Chem. Soc.* **2012**, *134*, 11968–11970; c) S. Bivaud, S. Goeb, V. Croué, P. I. Dron, M. Allain, M. Sallé, *J. Am. Chem. Soc.* **2013**, *135*, 10018–10021; d) V. Croué, S. Goeb, G. Szalýki, M. Allain, M. Sallé, *Angew. Chem. Int. Ed.* **2016**, *55*, 1746–1750; *Angew. Chem.* **2016**, *128*, 1778–1782; e) K. Yazaki, S. Noda, Y. Tanaka, Y. Sei, M. Akita, M. Yoshizawa, *Angew. Chem. Int. Ed.* **2016**, *55*, 15031–15034; *Angew. Chem.* **2016**, *128*, 15255–15258.

[9] a) B. Therrien, G. Süss-Fink, P. Govindaswamy, A. K. Renfrew, P. J. Dyson, *Angew. Chem. Int. Ed.* **2008**, *47*, 3773–3776; *Angew. Chem.* **2008**, *120*, 3833–3836; b) S. Mirtschin, A. Slabon-Turski, R. Scopelliti, A. H. Velders, K. Severin, *J. Am. Chem. Soc.* **2010**, *132*, 40, 14004–14005; c) B. Breiner, J. K. Clegg, J. R. Nitschke, *Chem. Sci.* **2011**, *2*, 51–56; d) G. Gupta, A. Das, N. B. Ghate, T. Kim, J. Y. Ryu, J. Lee, N. Mandal, C. Y. Lee, *Chem. Commun.* **2016**, *52*, 4274–4277; e) P. Rajasekar, S. Pandey, J. D. Ferrara, M. D. Campo, P. L. Magueres, R. Boomishankar, *Inorg. Chem.* **2019**, *58*, 15017–15020; f) A. Yadav, M. Sarkar, S. Subrahmanyam, A. Chaudhary, E. Hey-Hawkins, R. Boomishankar, *Chem. Eur. J.* **2020**, *26*, 4209–4213.

[10] a) J. Mattsson, P. Govindaswamy, A. K. Renfrew, P. J. Dyson, P. Stepnicka, G. Suess-Fink, B. Therrien, *Organometallics* **2009**, *28*, 4350–4357; b) N. P. E. Barry, O. Zava, P. J. Dyson, B. Therrien, *Chem. Eur. J.* **2011**, *17*, 9669–9677; c) S. Shanmugaraju, A. K. Bar, S. A. Joshi, Y. P. Patil, P. S. Mukherjee, *Organometallics.* **2011**, *30*, 1951–1960; d) V. Vajpayee, Y. H. Song, Y. J. Yang, S. C. Kang, H. Kim, I. S. Kim, M. Wang, P. J. Stang, K.-W. Chi, *Organometallics.* **2011**, *30*, 3242–3245; e) A. A. Adeyemo, S. Shanmugaraju, D. Samanta, P. S. Mukherjee, *Inorg. Chim. Acta.* **2016**, *440*, 62–68.

[11] S. Kanegawa, Y. Shiota, S. Kang, K. Takahashi, H. Okajima, A. Sakamoto, T. Iwata, H. Kandori, K. Yoshizawa, O. Sato, *J. Am. Chem. Soc.* **2016**, *138*, 14170–14173.

[12] Void volume calculations have been performed by using the MSRoll module built in X-seed program version 4.04. a) L. J. Barbour, *Chem. Commun.* **2006**, *42*, 1163–1168; b) L. J. Barbour, *J. Appl. Crystallogr.* **2020**, *53*, 1141–1146.

[13] a) A. Dei, D. Gatteschi, U. Russo, *Inorg. Chem.* **1991**, *30*, 2589–2594; b) M. E. Ziebel, L. E. Darago, J. R. Long, *J. Am. Chem. Soc.* **2018**, *140*, 3040–3051.

Manuscript received: April 7, 2021
Accepted manuscript online: May 12, 2021
Version of record online: June 1, 2021

